Applied Catalysis B: Environmental 178 (2015) 124–132

Contents lists available at ScienceDirect

Applied Catalysis B: Environmental

journal homepage: www.elsevier.com/locate/apcatb

Surface decoration of commercial micro-sized TiO_2 by means of high energy ultrasound: A way to enhance its photocatalytic activity under visible light

M. Stucchi[a,e,*], C.L. Bianchi[a,e], C. Pirola[a,e], S. Vitali[a], G. Cerrato[d,e], S. Morandi[d,e], C. Argirusis[b], G. Sourkouni[c], P.M. Sakkas[b], V. Capucci[f]

[a] University of Milan, Via Golgi 19, 20133 Milan, Italy
[b] National Technical University of Athens, Athens, Greece
[c] Energy Research Centre Lower Saxony, Goslar, Germany
[d] University of Turin & NIS Centre of Excellence, Turin, Italy
[e] Consorzio INSTM, Firenze, Italy
[f] GranitiFiandre SpA, Castellarano (MO), Italy

ARTICLE INFO

Article history:
Received 14 July 2014
Received in revised form
30 September 2014
Accepted 2 October 2014
Available online 13 October 2014

Keywords:
Photocatalytic activity
TiO_2
Visible light

ABSTRACT

Although the TiO_2 is one of the most promising materials for its photocatalytic potential related to the pollution abatement, it strongly suffers from the low photocatalytic activity if it is used under visible light and not under UV light. Among the various possible modifications, the surface decoration with metal or metal oxides NPs can be a good strategy to increase the potential of TiO_2 in the visible range. In this paper, a sonochemical method that exploits the use of high-energy ultrasounds is suggested to obtain this surface decoration. The support is a commercial and micrometric TiO_2, cheaper and easier to handling than the nanometric P25. Samples were tested on the photodegradation of toluene and acetone in a gas phase system, using both the UV and LED lamp.

1. Introduction

TiO_2 is the most widely investigated photocatalyst due to its high photo-activity, low cost, low toxicity and good chemical and thermal stability. It was first used for the remediation of environmental pollutants in 1977 and since then there was a dramatic increase of the research in this area because of the potential for water and air purification [1].

Titanium dioxide is typically an n-type semiconductor due to the oxygen deficiency. The band gap is 3.2 eV for Anatase: this is the main TiO_2 polymorph and it is the most active phase in terms of photocatalytic activity.

In photocatalysis, light of energy greater than the band gap of the semiconductor excites an electron from the valence band to the conduction band (e_{cb}^-) generating a positive hole in the valence band (h_{VB}^+): in the case of titanium dioxide, because of the 3.2 eV band gap, UV light is required. Positive holes can oxidize OH^- or water at the surface to produce •OH radicals, which are extremely powerful oxidants.

A lot of studies describe the negative effects on health related to the exposition to chemical pollutants, found in particular in the indoor environment [2–4]. The latter are classified in the VOC's (Volatile Organic Compounds) category, and most of them are toxic or carcinogenic. VOC's are chemical substances of different nature: it is important to underline that more than 300 species were detected in the indoor atmosphere, with a concentration from 2 to 10 times higher than in the outdoor one.

As modern people spend the most part of their time in the indoor environment, it is clear that the air quality of these places is a crucial point of priority interest [2,5].

Among many AOPs (Advanced Oxidation Processes), TiO_2 photocatalysis is one of the most viable environmental cleanup technology: even if TiO_2 needs to have a higher activity to be economically competitive, from a practical point of view alternative materials that are as advantageous as TiO_2 are hard to be found [6].

The recombination of photogenerated charge carriers is one of the main limitations in semiconductor photocatalysis, and the crucial problem related to the practical use of the TiO_2 is its inability to be active under the visible light. This problem becomes harder

* Corresponding author at: University of Milan, Via Golgi 19, 20133 Milan, Italy. Tel.: +39 3476000699.
E-mail address: marta.stucchi@unimi.it (M. Stucchi).

http://dx.doi.org/10.1016/j.apcatb.2014.10.004
0926-3373/

when one thinks about TiO_2 used in the indoor areas where the lighting system is moving towards the total use of LED lamps, which are UV-radiation free.

Therefore, the most important demand is the introduction of the visible light activity that is absent with pure TiO_2 [7]. In this sense, several modification methods were developed in order to accelerate the photoconversion, enable the absorption of visible light, and alter the reaction mechanism or control products and intermediates [8]. The surface deposition of metal or metal oxide nano-particles (NPs) can be useful because of many factors: metals onto the TiO_2 surface can enhance the electron transfer or the charge separation and improve the formation of the free hydroxyl radicals; it was shown that also metal oxide particles can have a positive effect because they support the charge separation and prevent their recombination [9,10].

The reason why the surface metal NPs affect the photochemical properties of TiO_2 is related to three main concepts: firstly, the UV radiation leads to a Fermi level shift, indicating an electron transfer at the interface that promote the photocatalytic reactions; another important aspect to take into account is the presence of free electrons in the metal particles that can be excited by light and finally the possibility that metals act as an electron sink promoting also in this case the charge separation.

Decoration of M- or MO-NPs is commonly implemented by means of ultra-sounds (US) in aqueous or organic solutions where ceramics or polymer substrate powders are dispersed [11]. The idea in this instance is to apply the same method using the micrometric TiO_2 as substrate, depositing on its surface species such as tungsten or rhenium oxide, molybdenum or copper. Because it was widely demonstrated that the TiO_2 surface modification can be useful to improve its photocatalytic activity, sonochemistry is a novel and interesting way to obtain the surface decoration of TiO_2 powder with metal nanoparticles. The sonochemical method described in this paper has been used for instance in the decoration of anode materials for Solid Oxide Fuel Cells (SOFC) [12].

Finally, it is important to underline that the substrate is micrometric TiO_2 and not the nanometric one: the upgrade of the micrometric TiO_2 is crucial because of the important drawbacks of the nanometer powders. The latter could be inhaled and come into direct contact with the cells of the organism; although the negative TiO_2 effects on human health were not fully demonstrated yet, some animals test have reported that TiO_2 nanoparticles are more dangerous than the micro ones and they have an higher influence to cancer, lung cancer in particular [13]. Based on the above mentioned, the use of micro-TiO_2 in order to take advantage from its photocatalytic properties is a challenging study to develop [14–16].

2. Experimental

2.1. Materials and characterization methods

TiO_2 1077 by Kronos is a micro-sized photocatalyst classified as pigment [15]. The main properties are summarized in Table 1.

For the sonochemical method, the precursor materials are purchased and used without further purification; they are $Mo(CO)_6$ (≥99.9% Sigma Aldrich), $Re_2(CO)_{10}$ (98% Aldrich), $W(CO)_6$ (99.99% Sigma Aldrich), and $CuCl_2{\cdot}2H_2O$ (≥99% Sigma Aldrich).

A Bandelin SONOPLUS HD 3200 utilizing a 200 W U/S generator and a sonication extension horn of 13 mm diameter generating US are employed.

In a 100 ml glass flask 0.25 g of $W(CO)_6$ or $Mo(CO)_6$ or $Re_2(CO)_{10}$ and 2 g (1 g for the decoration with Re) of Kronos TiO_2 are weighted; 100 ml of diphenylmethane are then added and the solution obtained is sonicated at a constant temperature of 80 °C for 3 h, with 33.0% amplitude and a 50 W cm^{-2} intensity. The $W(CO)_6$ solution changed colour from white to brownish. At the end the solution is centrifuged many times to remove all the solvent; the final powder is washed three times with n-pentane and centrifuged again, and one time with pentane and also in this case is centrifuged after washing. The residual solvent is evaporated and the sample is finally calcined at 480 °C for 40 h to completely remove the organic scents.

As for Kronos TiO_2 decorated with copper, a first solution with 3 g of L-ascorbic acid, 5 g of CTAB, 72 ml of H_2O and 2 g of Kronos TiO_2 is prepared. Then, a second solution with 1.5 g of $CuCl_2{\cdot}2H_2O$, 6 ml of NH_3 and 15 ml of H_2O in prepared. They are mixed and the solution obtained is sonicated at a set temperature of 62 °C for 2.5 h, with a 55.0% amplitude and a 100 W/cm^2. At the end, the sample is centrifuged in order to remove the solvent and it is washed with water. After washing, the powder is calcined at 480 °C for 40 h.

BET analysis was performed with a Sorptometer Instrument (Costech mod. 1042); the XRD spectra were collected using a PW 3830/3020 X' Pert Diffractometer from PANalytical working Bragg-Brentano, using the Cu $K_{\alpha1}$ radiation (λ = 1.5406 Å); TEM images were collected using the JEOL 3010-UHR Instrument (acceleration potential 300 kV; LaB_6 filament); the XPS characterizations were performed with a M-probe apparatus (Surface Science Instruments).

Absorption/transmission IR spectra were obtained on a Perkin-Elmer FT-IR System 2000 spectrophotometer equipped with a Hg-Cd-Te cryo-detector, working in the range of wavenumbers 7200–580 cm^{-1} at a resolution of 2 cm^{-1} (number of scans ~20). For IR analysis powder catalyst was compressed in self-supporting disc (of about 10 mg cm^{-2}) and placed in a homemade quartz cell, equipped with KBr windows, connected to a conventional high-vacuum line (UHV). Spectra were recorded at room temperature (RT) on the samples after prolonged outgassing at RT.

2.2. Photocatalytic tests

The photodegradation kinetics was performed using both a UV lamp (Jelosil–Model HG-500, 500 W, λ = 315–400 nm) and a LED lamp (MW mean well, 350 mA rated current, 9–48 V DC voltage range, 16.8 W rated power) with an emission between 400 and 700 nm. The pollutants concentration was monitored using a gas chromatography (Agilent 3000 A microGC).

3. Results

3.1. Sample characterization

As reported in Table 2, surface decoration has almost no effect on the surface area of the samples, but for the Cu-decorating sample for which a marked reduction of surface area is observed.

As evidenced in the XRD patterns reported in Fig. 1, surface decoration does not affect the structural properties of Kronos 1077. All

Table 1
Main features of the TiO_2 commercial sample.

Sample	Composition	Average crystallite size (nm)	SSA (m^2 g^{-1})	XPS	Band gap (eV)
1077 by Kronos	100% Anatase	110	12	Ti(IV)	3.15

Table 2
BET surface areas.

Sample	BET surface area ($m^2\ g^{-1}$)
1077 by Kronos (reference sample)	12
A (Kronos + W)	13
B (Kronos + Re)	13
C (Kronos + Mo)	12
D (Kronos + Cu)	4

the XRD patterns exhibit the presence of the peaks characteristic of the anatase phase [ICDD anatase file no. 21-1272]. In particular, for both W- and Re-containing samples XRD analysis puts in evidence that only the peaks related to anatase are present. Differently, in addition to these diffraction peaks, the XRD patterns of Cu- and Mo-containing samples show the presence of peaks related to CuO [spatial group C2/c, monoclinic phase, ICDD tenorite file no. 01-072-0629], Cu_2O [spatial group Pn3m, cubic phase, ICDD cuprite file no. 01-075-1531] and MoO_3 [spatial group Pbnm, orthorhombic phase, ICDD molybdite file no. 01-075-0912] phases, respectively. The presence of copper oxide phases is reasonably related to the loss of surface area observed for Cu-containing sample (Table 2).

TEM analysis shows that the bare Kronos 1077 is characterized by an average crystallites dimensions lying in the 100–150 nm range (see Fig. 2 TEM): the titania particles exhibit roundish contours and very clear fringes patterns, the detailed inspections of which always indicates the presence of anatase, in particular of the

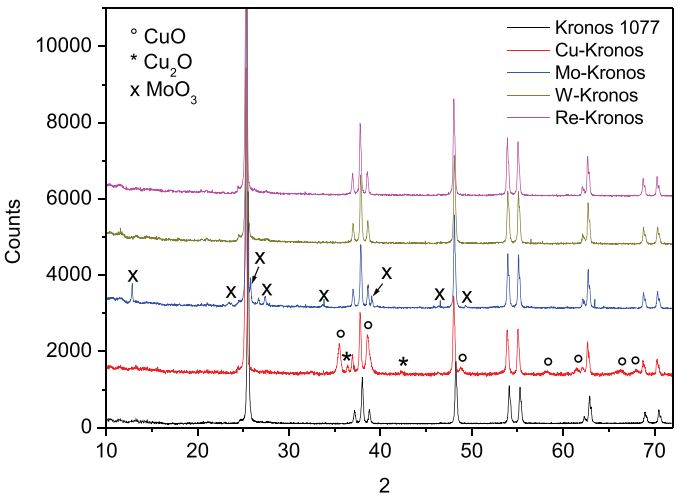

Fig. 1. XRD patterns of bare and decorated Kronos 1077.

(101) crystal planes [ICDD anatase file no. 21-1272]. If we compare this material with the reference nanometric TiO_2 system used in photocatalysis, i.e. P25 by Aeroxide Evonik, its very different morphology is evident (see Fig. 3) and is already discussed by Bianchi et al. [18].

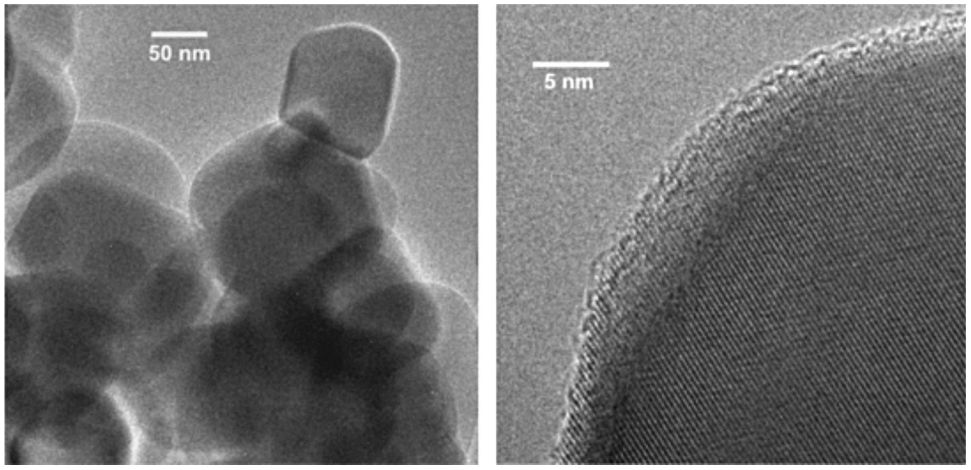

Fig. 2. TEM images of Kronos 1077.

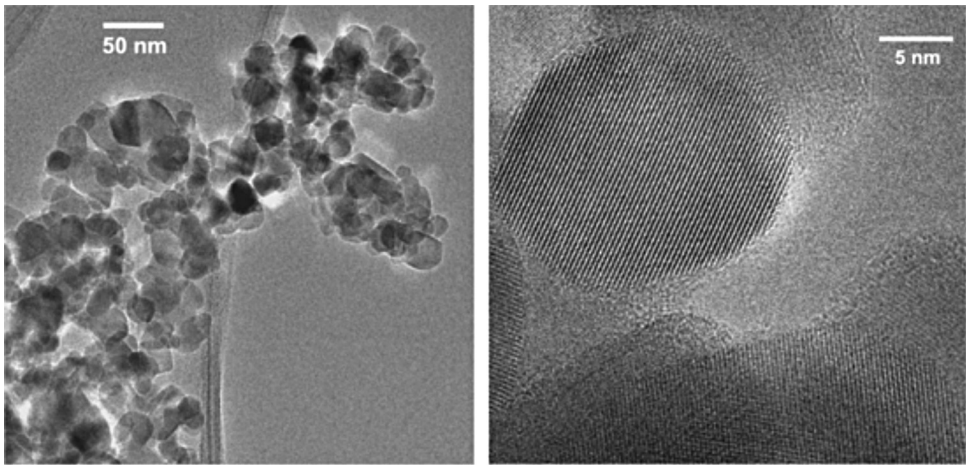

Fig. 3. TEM images of P25 by Evonik.

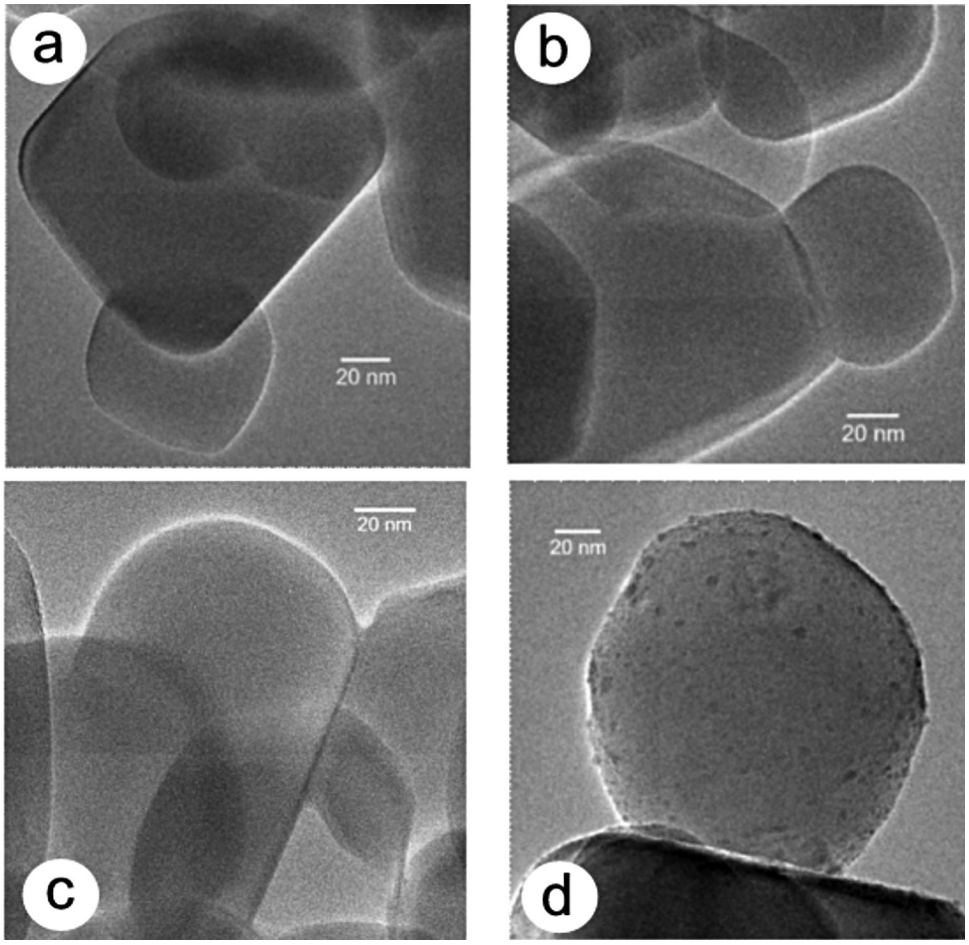

Fig. 4. Low magnification TEM images of all decorated systems. (a) Mo decorated Kronos; (b) Re decorated Kronos; (c) W decorated Kronos; (d) Cu decorated Kronos.

All the decorated materials have been investigated by means of HRTEM in order to shed some light onto their morphological habit.

At low magnification (Fig. 4), all decorated samples exhibit the main morphological features typical of the parent Kronos system, i.e. well ordered TiO_2 crystallites with almost unchanged average dimensions, in agreement with XRD results. This is totally true for Mo, W and Re decorated materials, whereas a few peculiarities can be put into evidence for the Cu decorated TiO_2. In fact, for the latter system a huge amount of small (nano) particles are present on top of the parent Kronos surface (see section d in Fig. 4). If in the latter case, the different external habit of the crystallites can be due to the presence of an extra species, for the other samples there is no indication of the presence of Mo, W or Re species. We then performed for all samples EDX analyses: in all cases, the presence of the extra species has been confirmed (data not reported of the sake of brevity).

Moreover, we carried out also a detailed inspection in high-resolution transmission electron microscopy (Fig. 5), in order to investigate the ultimate nature of the crystallites. For Re decoration the features typical of the parent Kronos system remain almost unchanged, whereas in the case of Mo, W and Cu addition remarkable changes are evident.

When W is present as decorating agent (see the top images reported in Fig. 5), a general loss of definition of the crystallinity of the TiO_2 particles is observed: the fringes patterns always well-defined for the Kronos system are now hardly evident. The same can be observed for Mo-containing sample (not reported). This might be due to the presence of either W or Mo in the form of oxide (or sub-oxide) covering the support particles as a thin "coating", and not in the form of metal, as the typical features of metallic W or Mo have been never evidenced. This is in agreement with XRD results obtained for Mo-Kronos that put well in evidence the presence of the MoO_3 phase. Otherwise, no W-phases were visible by XRD, reasonably either due to the amount under the detection limit of the technique or because in the form of an amorphous coating.

Table 3
XPS binding energy (eV) of the metal species from Handbook.

Copper—Cu	Tungsten—W	Rhenium—Re	Molybdenum—Mo
$2p_{3/2}$ = 933.6 eV	$4f_{7/2}$ = 31.4 eV	$4f_{7/2}$ = 40.3 eV	$3d_{5/2}$ = 228 eV
Δ = 19.9 eV	Δ = 2.2 eV	Δ = 2.4 eV	Δ = 3.1 eV

For all decorations carried out using Cu, its presence is well evident. In fact, many particles with the contrast typical of a metal are observed (see the bottom images in Fig. 5). The average dimensions of these particles lies in the "nano" range, as they measure 1 nm or less in diameter: nevertheless, in this case the fringes patterns described for the TiO_2 Kronos system are still observable.

XPS spectra are reported in Fig. 6. Each spectrum confirms the presence of the metal species (Table 3) on the Kronos surface.

In this spectrum (Fig. 7) it is possible to see the distribution of the tungsten peaks and in particular the most important is the peak "A" that refers to the WO_3 species (Table 4), in agreement with the results obtained by TEM analysis.

Fig. 8 refers to copper decorated Kronos: the main peaks denote to the species Cu, CuO and Cu_2S (Table 4) and the presence of Cu in metal form is demonstrated, in agreement with the results obtained with XRD and TEM analysis.

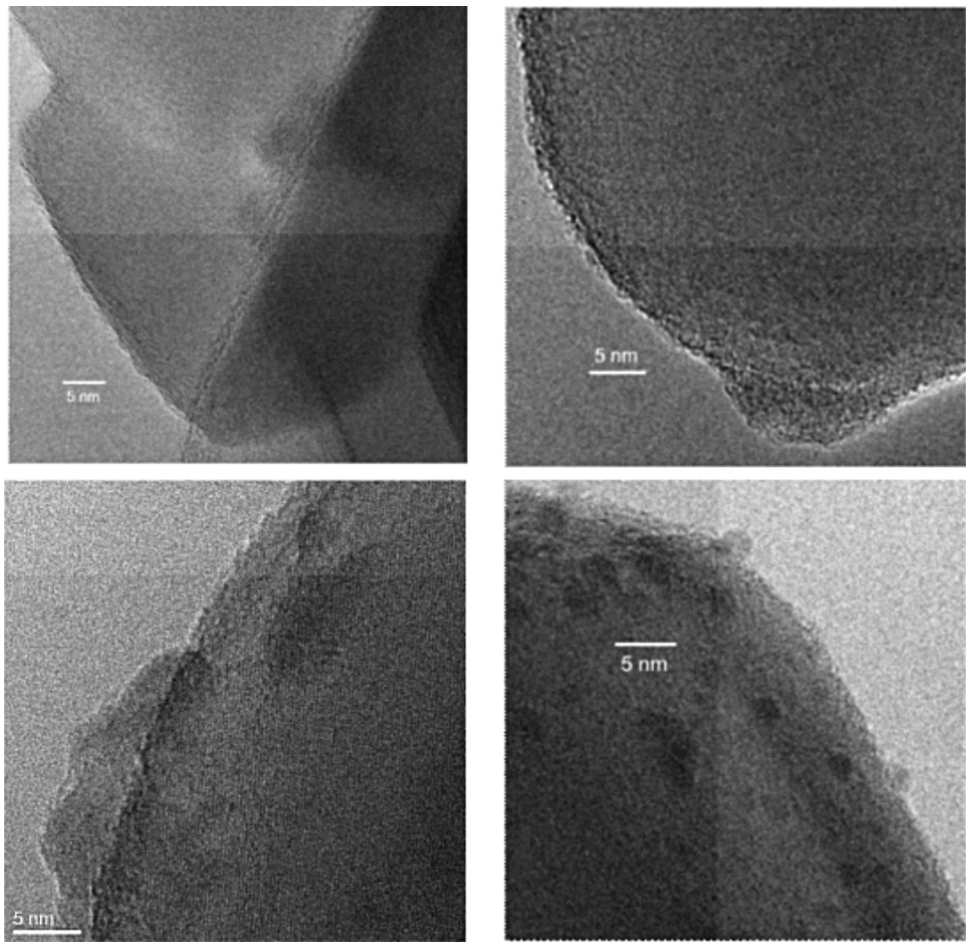

Fig. 5. TEM: High magnification TEM images of W (top images) and Cu (bottom images) decorated systems.

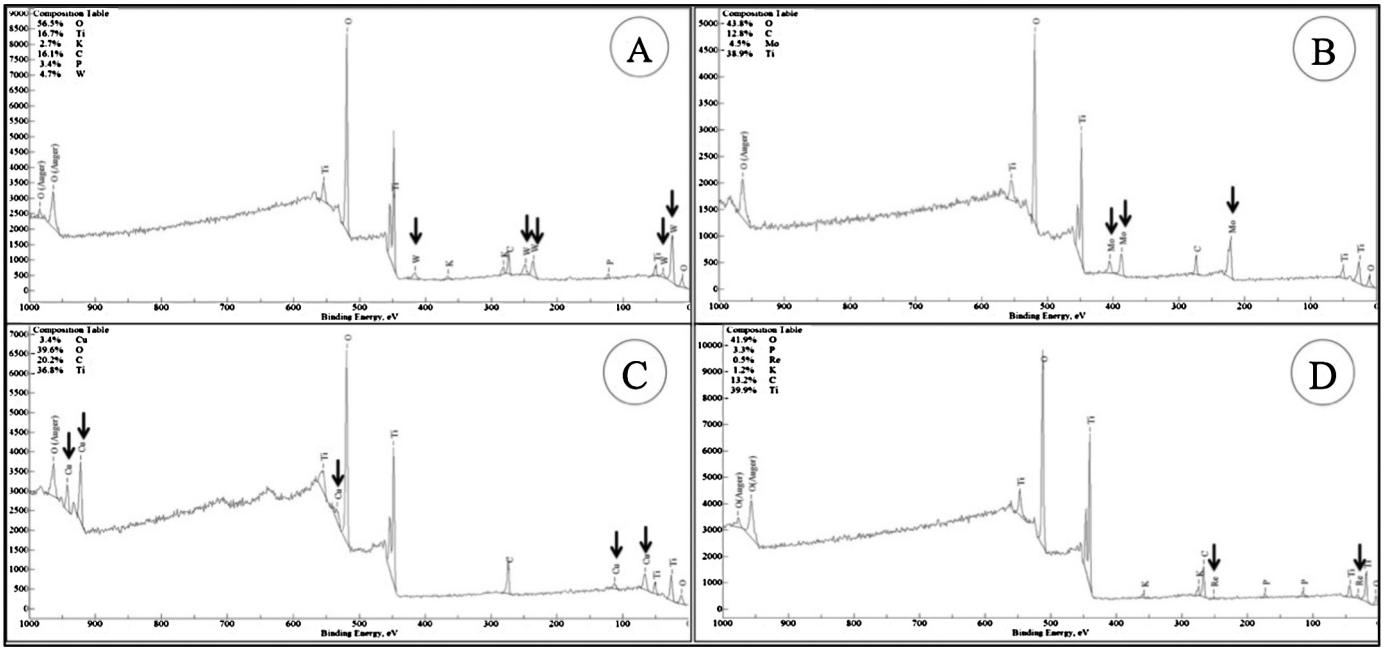

Fig. 6. XPS: Survey analysis. (A) W decorated Kronos; (B) Mo decorated Kronos; (C) Cu decorated Kronos; (D) Re decorated Kronos.

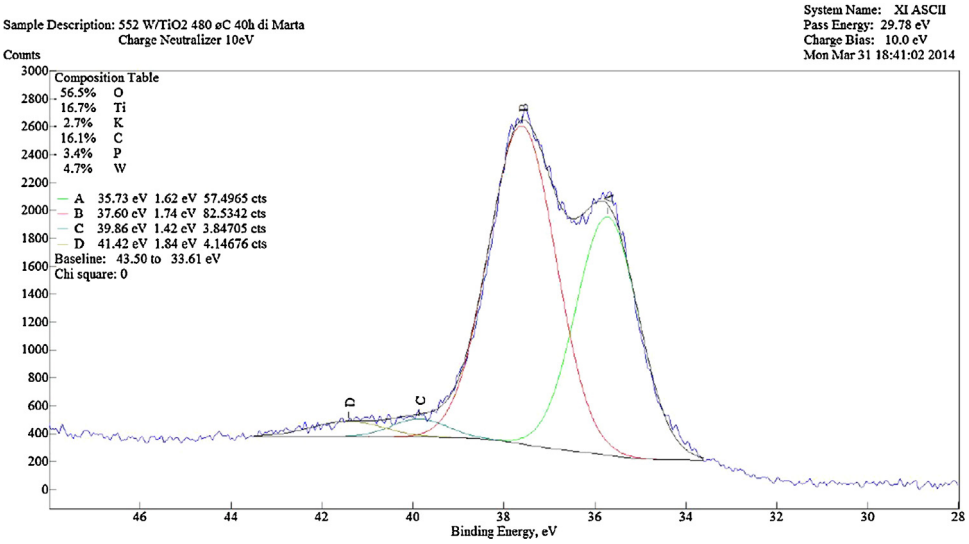

Fig. 7. XPS: W high-resolution spectrum.

Table 4
Summary data XPS spectra of all the synthetized samples.

Sample	Oxidation state	Binding energy (eV)	% $(M)^+$	$(M)^+$/Ti	OH/O
Ti-Cu	Cu^+ (Cu_2S); Cu^{2+} (CuO)	932.2 eV; 934.2 eV	3.4%	0.1	0.24
Ti-W	Oxides (WO_3); Tungstate	35.7 eV; 35.7 eV	4.7%	0.3	0.51
Ti-Re	Re^{6+} (ReO_3)	48.6 eV	0.5%	0.01	0.26
Ti-Mo	Mo^{6+} (MoO_3); Mo^{6+} (MoO_3)	232.4 eV; 235.5 eV	4.5%	0.1	0.09

As already discussed by Bianchi et al. [18], it was possible to evaluate the OH/O ratio for each decorated sample by means of the oxygen high-resolution spectra; the values measured for each sample are 0.51 for W decorated Kronos, 0.26 for Re decorated Kronos, 0.09 for Mo decorated Kronos and 0.24 for Cu decorated Kronos, respectively (Table 4).

The analysis of the surface hydroxyl groups was performed by collecting FT-IR spectra after prolonged outgassing at room temperature in order to remove physisorbed molecular water.

The spectra of samples prepared with Cu, Re and W show the typical peak related to the stretching mode of free hydroxyl groups of Kronos 1077 at 3670 cm^{-1} [19], while the spectrum of the sample prepared with Mo does not show it. This last finding can be related to the complete coverage of Kronos surface by a widely spread MoO_3 phase, whose presence has been put into evidence by XRD, TEM and XPS analysis. The copper-containing sample is characterized by other families of free hydroxyl groups reasonably related to CuO and Cu_2O phases, whose presence was already put into evidence by XRD and XPS analysis (Fig. 9).

3.2. Photocatalytic tests

In Fig. 10 the system scheme is reported.

The degradation reaction of toluene follows a multi-step path as is reported is Fig. 11, with the formation of different byproducts

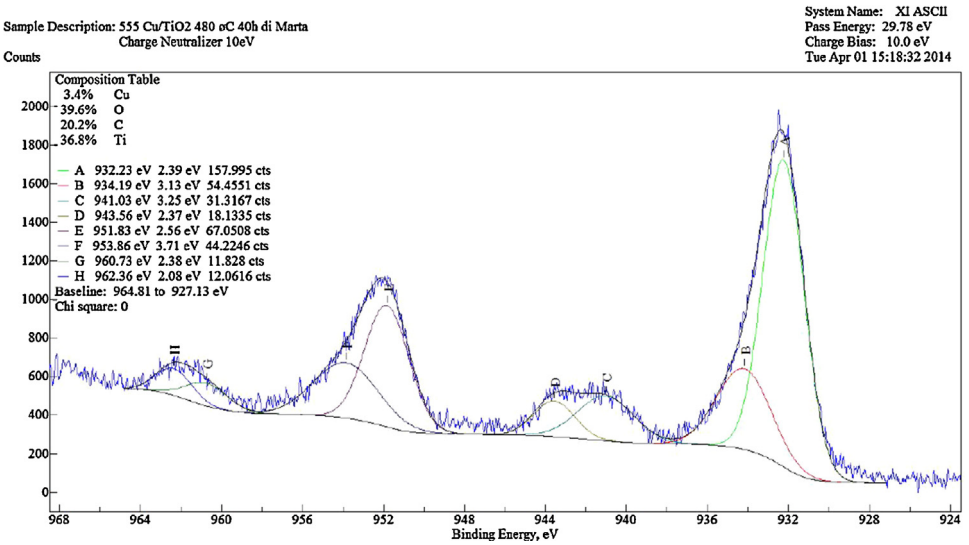

Fig. 8. XPS: Cu high-resolution spectrum.

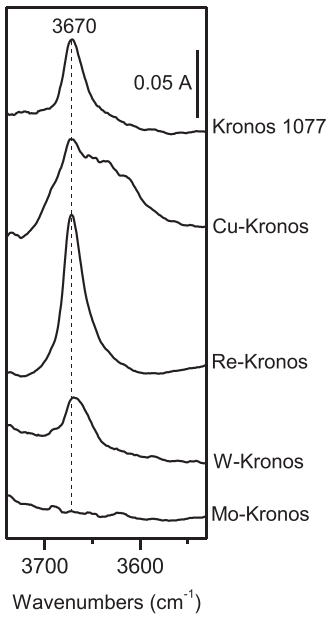

Fig. 9. FT-IR spectra.

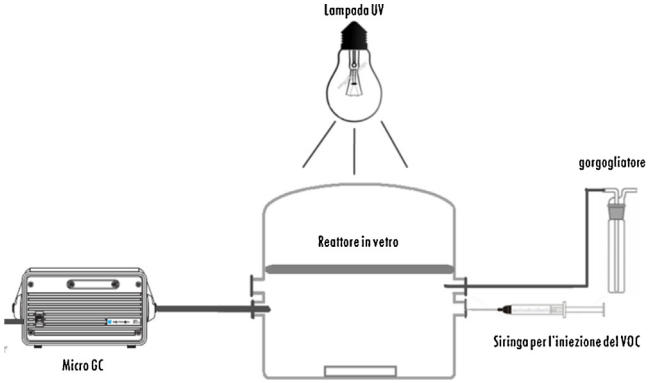

Fig. 10. Photoreactor gas-phase system scheme.

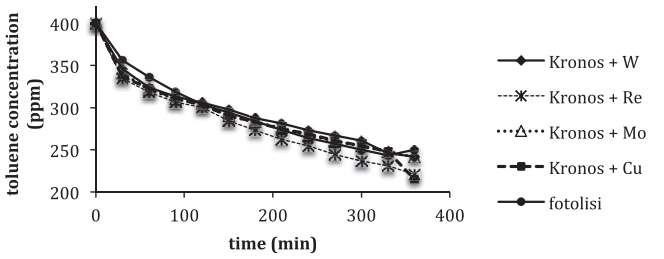

Fig. 12. Toluene photodegradation in gas-phase under UV irradiation [Toluene concentration] vs. time.

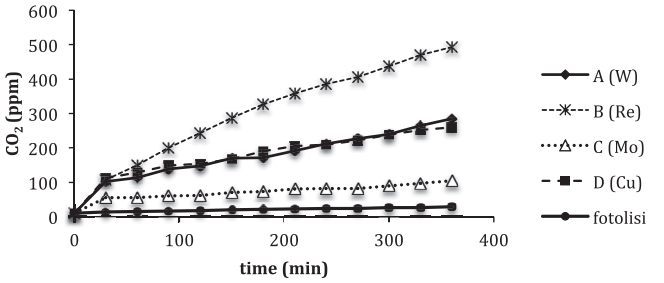

Fig. 13. CO_2 formation during the photodegradation process.

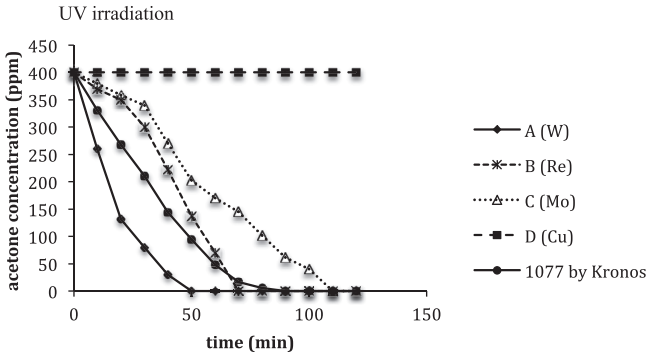

Fig. 14. Acetone photodegradation in gas-phase under UV irradiation.

before getting to the complete oxidation to CO_2 and water [18,20–23].

The samples were tested on the photodegradation of toluene firstly using the UV lamp (Figs. 12–15).

In case of the toluene degradation, apparently, the species put on the surface by the decoration do not increase the photocatalytic activity of the material; but they affect the byproducts' conversion into CO_2, so the surface decoration profitably acts on the byproducts, showing its concrete help in the degradation of the pollutant.

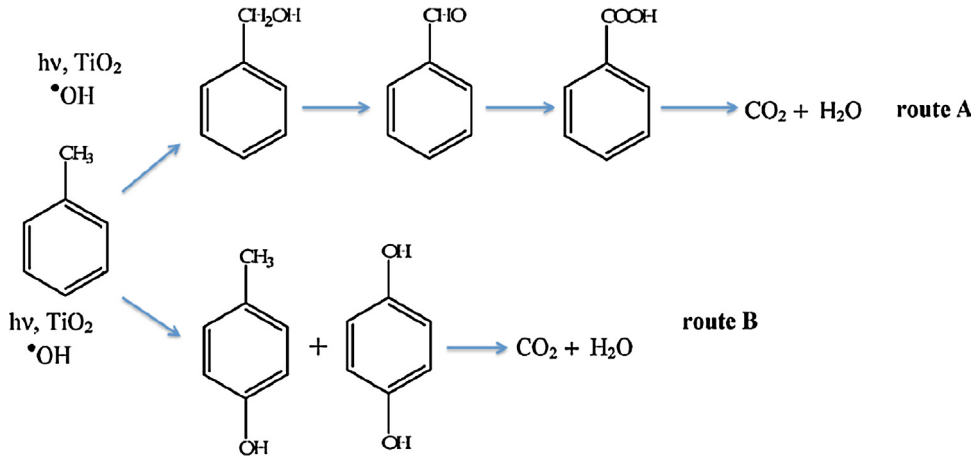

Fig. 11. Toluene oxidation reaction pathway [22].

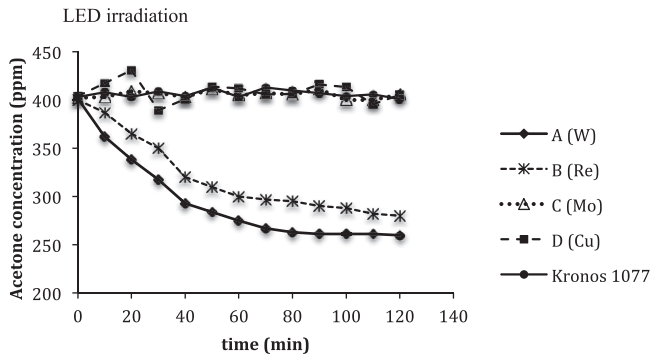

Fig. 15. Acetone photodegradation in gas-phase under visible light (performed with a LED lamp).

In particular, the Re-containing sample shows the highest CO_2 formation.

The tests on the acetone photodegradation were performed both with the UV lamp and the LED lamp. In this case the photolysis contribution in the photodegradation is negligible (less than 1%).

In case of acetone degradation, the effects of the surface decoration can already be seen directly on the degradation kinetic of the molecule, where the performances have definitely improved compared to Kronos 1077 results, in particular for W-containing sample. The presence of the tungsten oxide (WO_3) is confirmed in particular by the XPS analysis; moreover, in the TEM images it is possible to see that a thin film covers the Kronos surface, and it is tungsten oxide. Also the IR spectrum complies with this last information because the lower OH peak compared to Kronos is maybe due to the coating effect of tungsten oxide. All these concepts support the good results in the photodegradation tests because WO_3 is a semiconductor with known photocatalytic activity [24,25] and in this case it plays an important role in the degradation of the pollutant, justifying its effects. A complete loss of activity is observed in the case of the decoration of TiO_2 with Cu [17].

At least, using the LED lamp, without any UV radiation, it is clear that W and Re addition onto the TiO_2 surface plays a crucial role in the activation of the catalyst under the visible light. In fact, the bare TiO_2 is not able to work under visible light, because of the band gap of the TiO_2 which needs higher energy as delivered by the UV light.

The most apparent characteristic that could be related to the good activity of Re-decorating sample is the presence of a significant amount of free hydroxyl radicals, confirmed by the peak in the IR spectrum. Unfortunately, TEM images and XPS analysis are not so useful to evaluate the presence of rhenium in the oxide form, but the results are clearly a positive signal of a changing in the material properties necessarily due to the presence of the element.

If we take into consideration the chemical activity of the metal oxides themselves, the main concepts useful to explain the decorated TiO_2 behavior are the following: firstly, the presence of the metal oxides increases the "antenna effect"; the species on the TiO_2 surface are able to capture the electrons of the visible light, making them usable in the redox reactions that occur upon the surface. Secondly, it was shown that species like metal or metal oxides are able to act as an electron trap, reducing the electron–hole recombination rate [9,26].

The so-called "antenna mechanism" refers to the electrons or holes transfer between some particles in contact; the particle on the semiconductor surface can act as much as electrons trap as holes trap, and the immediate effect is a better electron–hole separation [27]. Surely, this photo-energy transfer from the location of light absorption to the local of reaction plays a significant role in all types of photocatalytic system [27].

This passage of electrons, assumed in the M-TiO_2 systems that are described in this paper, takes place thanks to the differences between the valence and conduction bands of the respective elements [28,29], and the sensitizer molecule must be anchored to the surface of the semiconductor [30].

In this paper, the visible-light activity of the samples prepared with Tungsten or Rhenium are shown: regarding the WO_3, with a band gap of 2.8 eV, it is able to absorb some portion of the visible light and it can be considered a sensitizer [31]. According to relative energy band positions between TiO_2 and visible-light-absorbing semiconductors, three different types of heterojunction can be described: in Type-A heterojunction, the conduction band (CB) level of sensitizer is positioned at a more negative side than that of TiO_2, whereas in Type-B system its valence band (VB) level is more positive than that of TiO_2 and in Type-C system the sensitizer energy level is located between the CB and VB of TiO_2 [28]. In particular, the TiO_2-WO_3 catalyst is classified as a type-b system [28]. Considering instead the sample containing Rhenium, the latter is also regarded as an "antenna-sensitizer" [30].

4. Conclusions

Through the innovations introduced by sonochemistry, it was possible to obtain this new type of surface decoration of a pigmentary micro-TiO_2, proving that this modification method can improve the photocatalytic activity of the material, in particular under the visible light, where pure TiO_2 is not an effective photocatalyst.

The most interesting species loaded on the TiO_2 surface are the tungsten oxide and the rhenium oxide because they have the best performances in terms of degradation of VOC's. Although the results obtained using the samples prepared with copper NPs are absolutely not good, it is highly likely that this is due to the to the amount of copper, so that samples decorated with different Cu content as the ones used in the present work should be prepared and tested in order to find the most useful loading.

It is possible to improve the photocatalytic activity of micro-sized TiO_2 (anatase) using decoration with different metal(oxide) nanoparticles, in particular under visible light, getting a very interesting product useful for the VOC's abatement and the consequent improvement of the air quality.

Acknowledgements

This research was supported by LIFE + Environment Policy and Governance project DIGITALIFE-LIFE13 ENV/IT/000140. The authors would like to thank Dr. D.G. Kanellopoulou, with Lab of Inorganic Materials Technology, NTUA, for all helpful regarding the samples preparation as well as Dr. V. Oldani and Dr. B. Sacchi for all the XPS measurements.

References

[1] M. Pelaez, N.T. Nolan, S.C. Pillai, M.K. Seery, P. Falaras, A.G. Kontos, P.S.M. Dunlop, J.W.J. Hamilton, J.A. Byrne, K. O'Shea, M.H. Entezari, D.D. Dionysiou, Appl. Catal. B: Environ. 125 (2012) 331–349.
[2] L. Curtis, W. Rea, P. Smith-Willis, E. Fenyves, Y. Pan, Environ. Int. 32 (2006) 815–830.
[3] Thomas Petry, Danielle Vitale, Fred J. Joachim, Ben Smith, Lynn Cruse, Reuben Mascarenhas, Scott Schneider, Madhuri Singal, Regul. Toxicol. Pharmacol. 69 (2014) 55–70.
[4] D. Saraga, S. Pateraki, A. Papadopoulos, Ch. Vasilakos, Th. Maggos, Building Environ. 46 (2011) 2333–2341.
[5] J. Heinrich, Int. J. Hygiene Environ. Health 214 (2011) 1–25.
[6] T. Ochiai, A. Fujishima, J. Photochem. Photobiol. C: Photochem. Rev. 13 (2012) 247–262.
[7] K.H. Leong, P. Monash, S. Ibrahim, P. Saravanan, Solar Energy 101 (2014) 321–332.
[8] Lyu Jinze, Zhu Lizhong, Burda Clemens, Catal. Today 225 (2014) 24–33.

[9] Hyunwoong Park, Yiseul Park, Wooyul Kim, Wonyong Choi, J. Photochem. Photobiol. C: Photochem. Rev. 15 (2013) 20.
[10] D.M. Tobaldi, A. SeverŠkapin, R.C. Pullar, M.P. Seabra, J.A. Labrincha, Ceram. Int. 39 (2013) 2619–2629.
[11] A. Gedanken, Ultrason. Sonochem. 14 (2007) 418–430.
[12] P.M. Sakkas, O. Schneider, G. Sourkouni, C. Argirusis, Ultrason. Sonochem. 21 (2014) 1939–1947.
[13] D. Yao, Z. Chen, K. Zhao, Q. Yang, W. Zhang, Proc. Environ. Sci. 18 (2013) 149–215.
[14] C.L. Bianchi, S. Gatto, C. Pirola, M. Scavini, S. Vitali, V. Capucci, Cement Concrete Comp. 36 (2013) 116–120.
[15] C.L. Bianchi, C. Pirola, F. Galli, G. Cerrato, S. Morandi, V. Capucci, Chem. Eng. J. (2014).
[16] G. Cerrato, C.L. Bianchi, S. Morandi, C. Pirola, M. Stucchi, M.V. Diamanti, M.P. Pedeferri, V. Capucci, Catal. Today—manuscript draft.
[17] B. Xin, P. Wang, D. Ding, J. Liu, Z. Ren, H. Fu, Appl. Surf. Sci. 254 (2008) 2569–2574.
[18] C.L. Bianchi, S. Gatto, C. Pirola, A. Naldoni, A. Di Michele, G. Cerrato, V. Crocellà, V. Capucci, Appl. Catal. B: Environ. 146 (2014) 123–130.
[19] D.A. Panayotov, J.T. Yates Jr., Chem. Phys. Lett. 410 (2005) 11–17.
[20] A. Di Paola, M. Bellardita, L. Palmisano, Z. Barbieriková, V. Brezová, J. Photochem. Photobiol. A: Chem. 273 (2014) 59–67.
[21] P. Du, A. Bueno-López, M. Verbaas, A.R. Almeida, M. Makkee, J.A. Moulijn, G. Mul, J. Catal. 260 (2008) 75–80.
[22] V. Augugliaro, S. Coluccia, V. Loddo, L. Marchese, G. Martra, L. Palmisano, Mario Schiavello, Appl. Catal. B: Environ. 20 (1999) 15–27.
[23] S.B. Kim, H.T. Hwang, S.C. Hong, Chemosphere 48 (2002) 437–444.
[24] Y. Liu, C. Xie, H. Li, H. Chen, T. Zou, D. Zeng, J. Hazard. Mater. 196 (2011) 52–58.
[25] R.A. Carcel, L. Andronic, A. Duta, Mater. Character. 70 (2012) 68–73.
[26] A. Kubacka, M.J. Mun, M. oz-Batista, M. Ferrer, Fernández-García, Appl. Catal. B: Environ. 140–141 (2013) 680–690.
[27] C. Wang, R. Pagel, J.K. Dohrmann, D.W. Bahnemann, C. R. Chim. 9 (2006) 761–773.
[28] S.B. Rawal, S. Bera, D. Lee, D. Jang, W. In Lee, Catal. Sci. Technol. 3 (2013) 1822.
[29] S.B. Rawal, A.K. Chakraborty, Y.J. Kim, H.J. Kim, W. In Lee, RSC Adv. 2 (2012) 622–630.
[30] C.A. Bignozzi, R. Argazzi, J.R. Schoonover, G.J. Meyer, F. Scandala, Solar Energy Mater. Solar Cells 38 (1995) 187–198.
[31] S. Shamaila, A.K.L. Sajjad, F. Chen, J. Zhang, J. Colloid Interface Sci. 356 (2011) 465–472.